Pergamon

0042-6989(94)00146-4

Vision Res. Vol. 35, No. 4, pp. 529–538, 1995

0042-6989/95 $9.50 + 0.00

Fourth Purkinje Image Signals Reveal Eye-lens Deviations and Retinal Image Distortions During Saccades

HEINER DEUBEL,* BRUCE BRIDGEMAN*†

Received 7 January 1994; in revised form 16 June 1994

Saccadic eye movements of various sizes and directions were registered simultaneously with the scleral search coil and a fifth-generation Dual Purkinje image eyetracker. Comparison of the search coil and the Purkinje image tracker records reveal considerable dynamic deviations during and immediately after the saccade, which we ascribe to the movements of the eye lens relative to the optical axis of the eye. Due to the increased stiffness of the tissues these deviations are smaller in older subjects. Also, they are larger at near accommodation. The size of the retinal image displacement which results from the lens movement proper can be as large as 0.5 deg, which may not be negligible in a number of visual tasks.

Saccade Lens Accommodation Purkinje image

INTRODUCTION

During saccadic eye movements the eye undergoes rapid accelerations, reaching over 20,000 deg/sec^2 for a 10 deg saccade (Bahill, Brockenbrough & Troost, 1981) and even greater values for larger saccades. It has generally been assumed that the eye rotates as a whole during these accelerations. With the assumption of an inelastic eye, motions of the retina across the visual image can be inferred directly from motions of the limbus or the pupil.

We present evidence here that the eye is not inelastic during saccades, and specifically that saccadic accelerations result in significant deviations of the lens from the optical axis. During the initial acceleration phase of the saccade, the lens lags behind the rest of the eye. It is held in place only by the fibres of the zonule of Zinn; these fibres must be elastic to allow accommodation to take place. At the start of a saccade the zonule begins a lateral movement, amounting to about 0.2 mm for each degree of rotation. This creates a lateral force on the lens, accelerating it after a delay. Peak acceleration, and peak elastic stress, occur after about one-quarter of the saccade duration. During the second half of the saccade there is an opposite peak of acceleration during which the lens movement is slowed by the elastic zonule. The lens overshoots the final eye position, and is pulled back by passive elastic forces.

The magnitudes of these effects are dependent on the elasticity of the zonule and of the lens. In older eyes, the effects should be reduced due to the increased stiffness of the accommodative system. Further, the lens of the young eye at near accommodation may be flattened by the zonule fibres during saccadic accelerations, briefly creating a more distant accommodative state during a saccade. The previous accommodative state would be restored by passive forces at the end of the saccade.

Observations suggesting sluggish eye-lens suspension had already been made in the last century. First, von Hess (1896) described a downward displacement of the lens with strong accommodation, which can be seen entoptically. This displacement, which can attain 0.3 mm, shows the effect of the weight of the eye lens poorly held in place by the relaxed zonula. Coccius (1888) observed the fourth Purkinje image and described a trembling of the lens with head movements.

To measure possible effects of eye elasticity in the vicinity of saccadic eye movements, we compare records from a limbic search coil (Robinson, 1963) and from a fifth-generation Dual-Purkinje image tracker (Crane & Steele, 1985), recorded simultaneously during the same saccade. The search coil provides a very accurate and kinematically well-resolved record of limbus position. The Purkinje-image tracker, however, records systematic deviations from the trajectories of saccades as measured with the search coil or with infrared techniques. Typically, the tracker records an overshoot at the end of each

*Max-Planck-Institut für Psychologische Forschung, Leopoldstrasse 24, 80802 München, Germany [*Fax* 49 89 34 24 73].
†Permanent address: Department of Psychology, University of California—Santa Cruz, Kerr Hall, Santa Cruz, CA 95064, U.S.A.

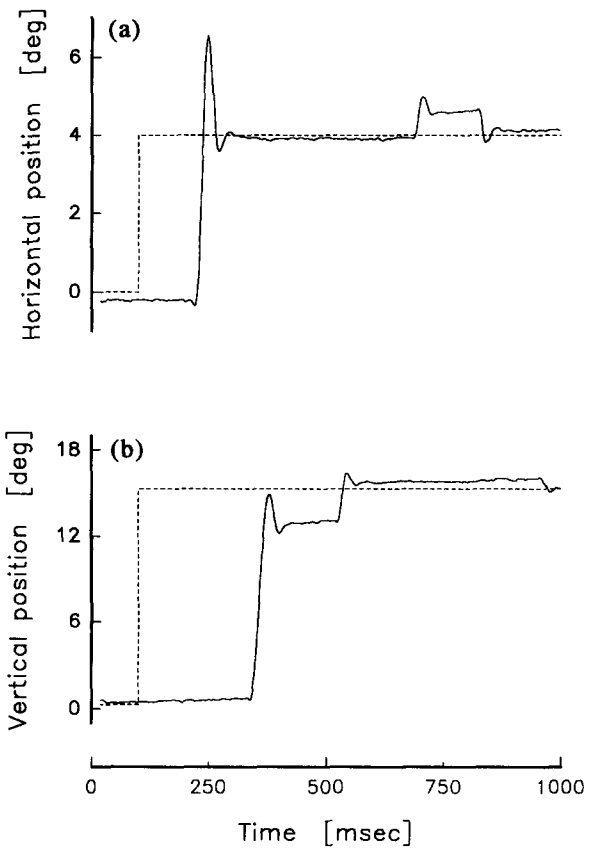

FIGURE 1. Saccades recorded with the fifth-generation dual-Purkinje image eyetracker. Dashed line, stimulus; solid line, eye tracker records. (a) Horizontal saccade to a 4 deg target step. (b) Vertical saccade to a 15 deg target step. The saccades show a small backshoot as well as an overshoot. The record also shows that overshoots occur in small as well as large saccades.

saccade (Fig. 1; Crane & Steele, 1978). This is not an artifact, for the bandpass of the fifth-generation tracker at about 400 Hz is adequate to follow both of the acceleration phases of the eye with minimal error even during saccades of 12 deg or more. (Earlier trackers were unable to follow the fourth Purkinje image during saccades of more than about 5 deg.)

We have also observed other deviations between the kinematics of coil and tracker records. At the beginning of a saccade the tracker records a small deviation in the direction opposite the eventual saccade direction, and the peak velocity of the saccade is nearly twice the velocity measured with the coil. We measure the characteristics of both the initial deviation, which we call a "backshoot", and the final overshoot. The deviations between the Purkinje image records and the coil records enable us to estimate the amplitudes and kinematics of retinal image motions that can be ascribed to the movements of the lens relative to the optical axis of the eye.

The study has two phases: comparison of search coil and Purkinje image tracker records of the same eye movements; and analysis of the backshoots and overshoots in the Purkinje-image tracker records.

METHODS

Apparatus

Search coil. Eye movements were recorded with a two-dimensional search coil based on the principle of Robinson (1963). Three sets of magnetic coils mounted orthogonally in a cubic coil frame (70 cm frame size along an edge) are driven with high-frequency alternating current (20 kHz) in phase quadrature, inducing currents in a small coil embedded in a toroidal contact lens (Skalar Medical, Delft). The lens is held firmly in place on the saddle-shaped surface at the edge of the limbus of the eye. The induced currents are recorded from two fine wires emanating from the search coil. After amplification and phase-locked detection two analogue signals are obtained which represent the sine of the horizontal and vertical components of the contact lens orientation. The system is insensitive to head translations within the region of uniform field. The system provides a noise level better than 1 min arc peak-to-peak at a bandwidth of 200 Hz, and a linearity error of $<0.25\%$.

Purkinje image tracker. Simultaneous with the search coil records, saccades were recorded with a fifth-generation dual Purkinje image eye tracker, based on a principle originally developed by Cornsweet and Crane (1973). The device projects a focussed infrared light source into the eye, and tracks both the first Purkinje image (the reflection from the front surface of the cornea) and the fourth Purkinje image (the reflection from the back surface of the lens). As the eye rotates, the first Purkinje image moves in the same direction as the eye, while the fourth image, from the concave surface of the back of the lens, moves in the direction opposite the eye (relative to the optical axis). Thus coincident movement of both images indicates head motion, while the difference between the two image motions indicates eye rotation. Special-purpose servomechanics allows a frequency response better than 250 Hz and a noise level equivalent to about 20 sec arc r.m.s. (Crane & Steele, 1985). Unlike earlier eye trackers, the fifth-generation device can follow saccadic movements of 15 deg or more without losing the eye.

Due to the elastic attachment of the eye lens, the lens is likely to lag the rotation of the eye axis at the beginning of the saccade, and to overshoot at the end of the saccade. These relative movements lead to artifacts in the Purkinje eyetracker records that follow from the geometrical properties of the eye. As shown in the Appendix, these calculations allows us to provide estimates of the dynamics of lens displacements from the tracker records.

Artificial eye. The Purkinje image tracker was calibrated with a special-purpose artificial eye positioned in the same location as the subject's eye. The artificial eye has glass reflective surfaces in the same positions (relative to the centre of rotation) as the first and fourth Purkinje image surfaces in a biological eye. It is rotated by a servo motor with a bandwidth of about 400 Hz.

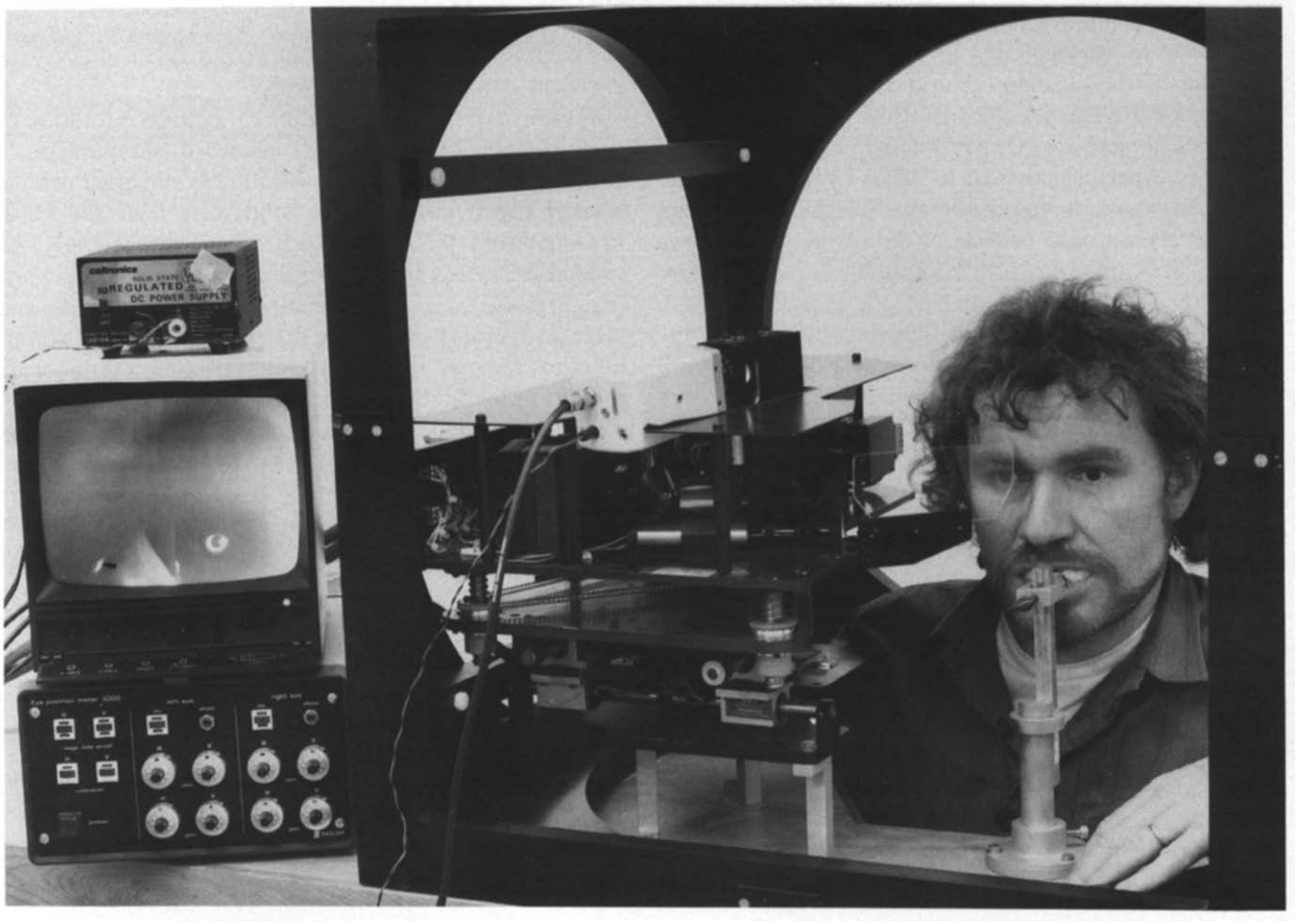

FIGURE 2. One of the authors serving as a subject. The picture shows the coil frame placed over the fifth-generation dual-Purkinje image eyetracker. The video monitor on the left displays the image of the pupil with the Purkinje reflections. The subject wears a scleral search coil in his right eye and follows stimuli presented on a computer screen.

Procedure

Simultaneous coil and tracker measurements. The cubic coil frame was placed over the Purkinje tracker so that the calibrated regions of both devices overlapped (Fig. 2). We verified that the insertion of the Purkinje eyetracker in the magnetic field of the search coil system had no noticeable effect on the signals induced in the eye coil. Also, we observed no effect of the electromagnetic field on the Purkinje signals. The head of the subject was stabilized with a bite bar and a forehead rest so that the right eye, equipped with the search coil, was located in this overlap region. Both the signals from the search coil system and the Purkinje eyetracker were digitized at 1 kHz for later analysis. The search coil and the Purkinje eyetracker were carefully calibrated by letting the subjects sequentially fixate locations indicated by little crosses on the screen. Based on these signals, an on-line calibration routine estimated veridical eye position. For the search coil signals, the routine was able to compensate for eventual rotations of the magnetic field that could have occurred due to an influence of the large metal parts of the Purkinje eyetracker. Both systems behaved linearly in the measuring range. For this and subsequent experiments, subjects tracked a small bright point target displayed on the computer screen as it jumped with variable and unpredictable amplitude and latency.

Verification of the eyetracker response. To examine the accuracy and dynamic behaviour of the Purkinje image tracker with biologically realistic signals, the digitized saccade records from the search coil were transformed back into an analogue signal and were used to drive the servo motors of the artificial eye with an angular amplitude and speed that matched that of the originally recorded saccades. The response of the tracker to these saccades, with the range and dynamic characteristics of normal saccades, was compared with the search coil records.

Overshoot and backshoot measurements. Samples of saccades were collected with the Purkinje image tracker at two target distances (corneal surface to screen surface): 22 cm, the closest that the apparatus would allow, and 390 cm, with the targets projected on the back wall of the laboratory. These distances represent accommodative states of 4.5 and 0.26 D respectively. We measured the differences in size and duration of backshoots and overshoots that resulted from this 4.24 D difference in accommodation, with the hypothesis that near accommodation would reduce the tension in the zonule fibres holding the lens and would result in larger overshoots and backshoots. We also collected samples of

saccades at an intermediate distance, 80 cm, in a number of subjects of varying ages to test the hypothesis that stiffening of the accommodation system would reduce mobility of the lens in older subjects.

Statistical methods. Simple (one-way) regressions and *t*-tests were performed with the STATVIEW program. The *t*-tests required equal domains for the saccades on which overshoot and backshoot data were based, since saccade size and over- and backshoot size were correlated. When the saccade domains for a test were unequal, the trials with saccades that deviated most from the mean of the combined distributions were discarded until the domains were similar. This never involved discarding more than three trials.

RESULTS

The Purkinje tracker's response to the artificial eye's saccades coincided precisely with that of the coil (Fig. 3). To assure that a brighter fourth Purkinje image from the artificial eye was not improving the tracker records over what would be expected from a biological eye, we repeated the observation with a 25% transmittance filter inserted into the optical path registering the fourth Purkinje image. The result was identical. We conclude that the backshoots and overshoots in the tracker records were not caused by oscillations of mechanical components or electrical circuits in the tracker, and that the eyetracker was able to follow the artificial eye with excellent dynamics and linearity.

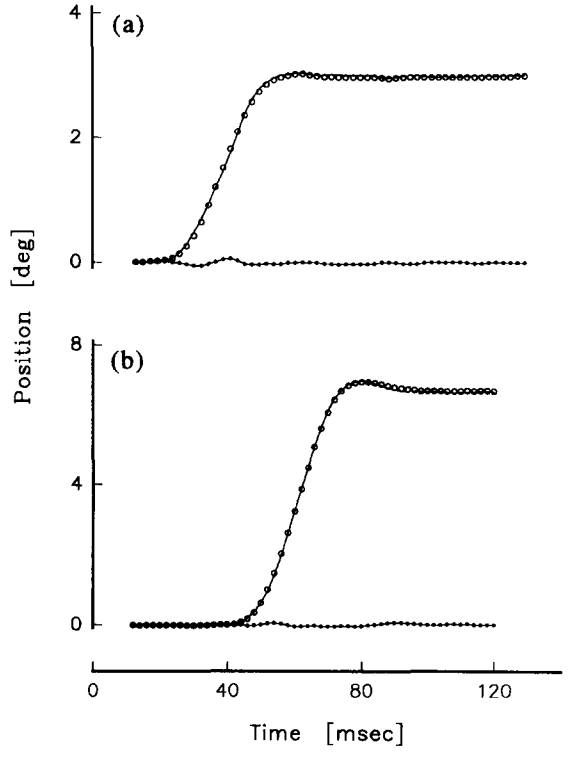

FIGURE 3. Natural saccades recorded with the scleral search coil (solid lines), with superimposed records of Purkinje eye tracker signals (open circles) from measurements of the same eye movement fed back into an artificial eye. The servo motor that rotated the artificial eye was fed with analogue values from a D/A converter reading out the eye movements recorded by the search coil. The differences are nearly unmeasurable (solid circles).

Figure 4 provides examples of natural saccades of various sizes and directions recorded simultaneously with the scleral search coil (solid lines) and the Purkinje tracker (open circles). The solid lines near the baseline represent the difference between both signals. As expected, records from natural saccades in the Purkinje image tracker displayed small initial backshoots and large overshoots even though, according to the simultaneous records from the coil, no such events were present in the limbus movements for the same saccades. The Purkinje signal follows the onset of the saccade only after a considerable delay, then overtakes the eye movement reaching velocities almost twice as high as the true eye rotation, finally ending in a prominent overshoot. The largest overshoots were in the range of 5 deg. In some subjects, we observed even multiple oscillations of the Purkinje tracker signal after the end of the saccade, indications of which are given in Figs 1(a) and 4(c). Further, it is interesting to note that the peak of each overshoot coincides approximately with the time of the conclusion of the coil-measured saccade. This suggests that the time of the maximum of the Purkinje tracker overshoot represents a practicable estimator for the veridical end of the saccade.

Overshoots

In separate sessions we recorded saccades in two subjects at each of the two accommodation states, 4.5 D (near) and 0.26 D (far), with the Purkinje tracker. Both subjects were in their early twenties, with normal ocular motility. Results for the two subjects were similar; average results will be given for the two subjects, with statistical tests given separately for each.

Figure 5 displays magnitudes of overshoots (a, b) and backshoots (c, d) in subjects IN (a, c) and AM (b, d). Straight lines are linear regressions, performed separately for near (solid lines) and far (dashed lines) accommodations. No regression lines are plotted where there was no statistically significant relationship of backshoot to saccade magnitude. For the far-accommodated saccades, simple regression analyses showed that overshoot magnitudes were statistically related to the sizes of the corresponding saccades [$F(1,48) = 49.6$, $P = 0.0001$; $F(1,78) = 31.3$, $P = 0.0001$]. Larger saccades tended to be accompanied by larger overshoots. Mean overshoot size corresponded to 0.94 deg of visual angle, for saccades averaging 5.79 deg and ranging from 0.26 to 15.85 deg. Since each degree of apparent deviation of the fourth Purkinje image corresponds to about 0.1 deg of image displacement on the retina (see Appendix; Crane & Steele, 1978), this corresponds to an average deviation of 0.094 deg (5.6 min arc) of the retinal image beyond that recorded from the coil at the end of each saccade. Even for medium-sized saccades the overshoots could be as large as 5 deg, presumably resulting in retinal image deviations of half a degree from the positions indicated by the limbus orientation.

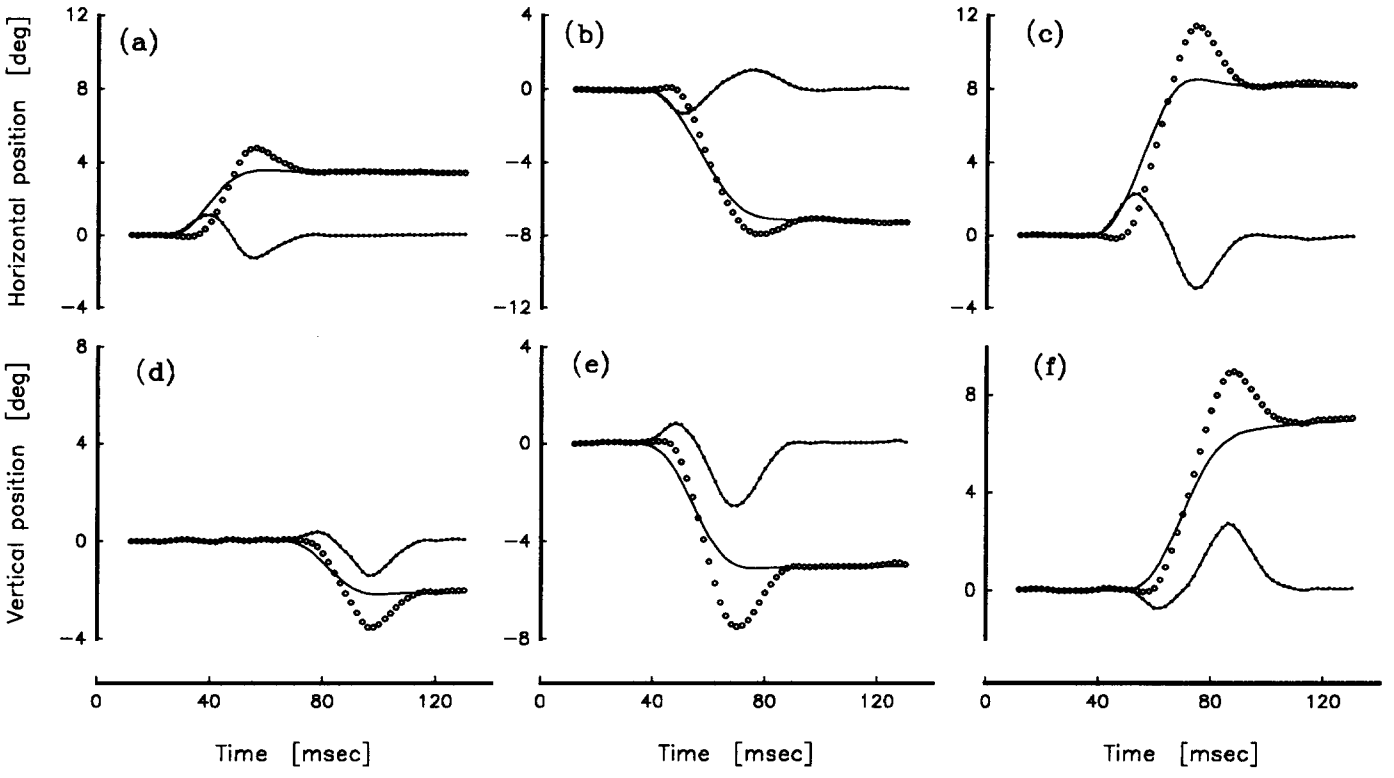

FIGURE 4. Saccades of different sizes recorded simultaneously by the search coil (solid lines) and the Purkinje eyetracker (open circles) along with their differences (solid lines near the baseline). The difference measure shows that the initial error and the final error are in opposite directions, and that the peak measured slope (peak velocity) of the saccade from the Purkinje tracker is greater than the slope measured with the search coil. Upper traces, horizontal saccades; lower traces, vertical saccades. Subject IN, viewing distance 80 cm.

At near accommodation the saccades averaged 6.1 deg, ranging from 0.41 to 16.04 deg. Mean overshoot size was 1.30 deg, corresponding to an overshoot of the retinal image of 0.13 deg (7.8 min arc) beyond that measured by the coil. The statistical significance of the difference in overshoots at the two accommodative distances was measured with a t-test: in both subjects, overshoots were significantly larger at near accommodation [$t(93) = 2.83$, $P = 0.0057$; $t(192) = 2.93$, $P = 0.0038$, discarding three outliers more than 3 SD from the mean of each distribution]. Some of this difference, however, may have been due to the fact that mean saccade size was larger at the near distance than at the far distance. Removing the effects of the difference in saccade size for subject IN, we reduced the mean saccade size for the near sample to 5.91 deg. The significance of the difference in overshoot sizes was nearly unchanged [$t(92) = 2.70$, $P = 0.0083$]. The relation between overshoots and saccade sizes is further supported by a difference in overshoots in the leftward and rightward directions. The two directions were analysed separately in subject AM, who had a larger data set. Rightward (abducting) saccades were faster, and showed significantly larger overshoots [$t(33) = 7.55$, $P = 0.0001$, again adjusting for equal saccade domain].

We conclude that near accommodation allows the lens to move more freely within a more relaxed set of zonular fibres, resulting in larger movements relative to the globe during saccades. A similar observation was recently reported by van Rensbergen, De Troy, Cavegn, De Graf, van Diepen and Fias (1993).

Backshoots

Backshoots were much smaller than overshoots [Fig. 5 (c, d)]. At far accommodation their mean magnitude was 0.09 deg, but backshoot magnitude was still significantly related to the magnitudes of the corresponding saccades [$F(1,49) = 11.59$, $P = 0.0013$] in one subject and marginally significant in the other [$F(1,78) = 4.59$, $P = 0.035$]. At near accommodation the backshoots were larger, averaging 0.15 deg, but they were related to saccade size in only one subject [$F(1,48) = 0.043$, $P = 0.84$; $F(1,121) = 5.1$, $P = 0.026$]. The difference between the magnitudes of backshoots at the two accommodative distances was statistically significant [$t(99) = 2.75$, $P = 0.007$; $t(201) = 6.44$, $P = 0.0001$].

Peak shapes

The durations of overshoots were significantly related to their magnitudes (Fig. 6) both at near accommodation [$F(1,48) = 23.69$, $P = 0.0001$; $F(1,121) = 21.88$, $P = 0.0001$] and at far accommodation [$F(1,48) = 6.93$, $P = 0.011$; $F(1,78) = 4.14$, $P = 0.0001$]. This is the

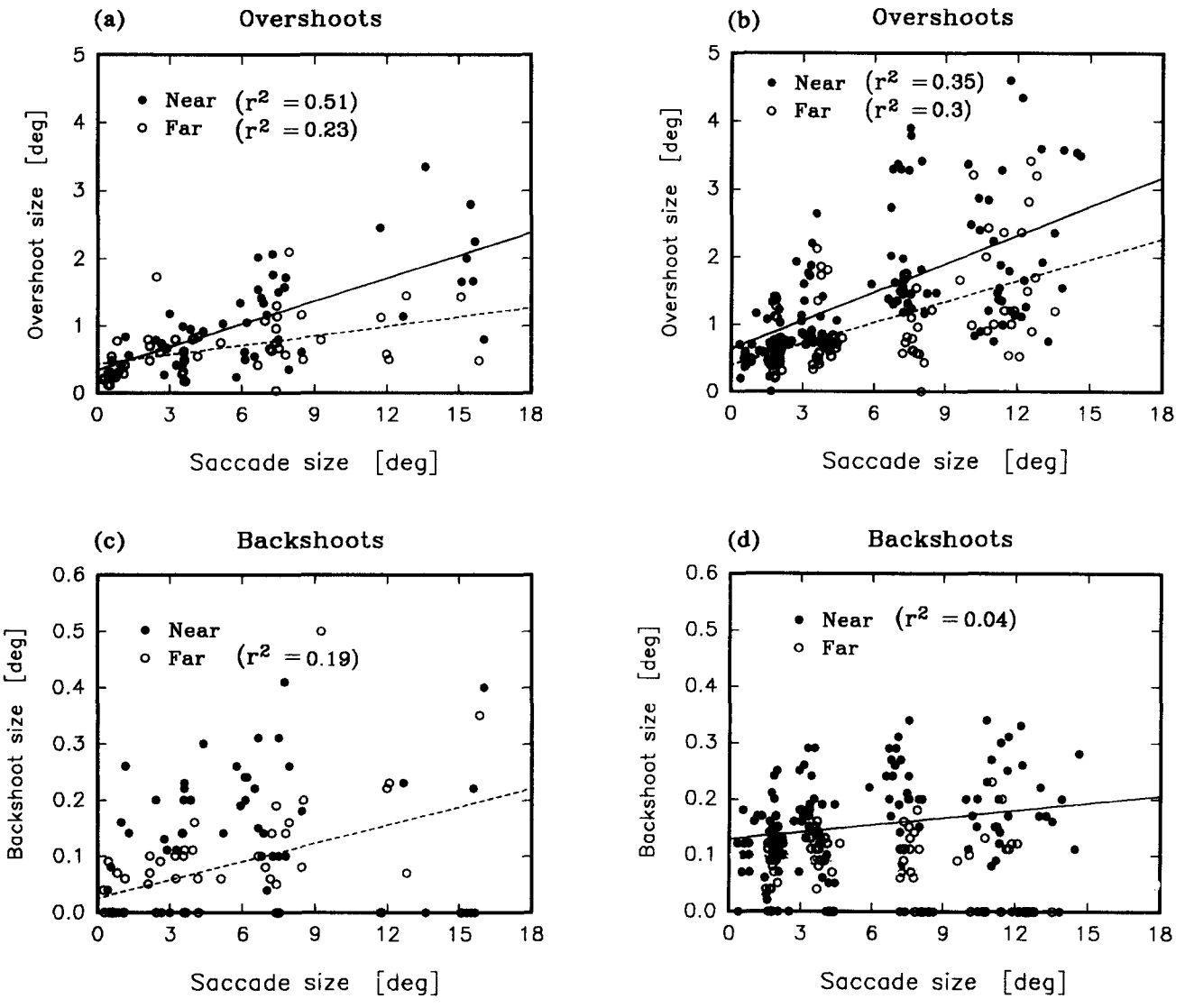

FIGURE 5. Magnitudes of overshoots (a, b) and backshoots (c, d) in subjects IN (a, c) and AM (b, d). Data are given separately for the viewing distances of 22 cm (solid circles, near) and 390 cm (open symbols, far). Straight lines are linear regressions, performed separately for near (solid lines) and far (dashed lines) accommodations.

expected behaviour of a spring working through both viscous and elastic loads. The same property was seen for the backshoots, with an even larger change of duration with size [$F(1,48) = 73.76$, $P = 0.0001$; $F(1,121) = 131.7$, $P = 0.0001$ at near; $F(1,49) = 85.33$, $P = 0.0001$; $F(1,78) = 203.8$, $P = 0.0001$ at far].

Relationship of dynamics with age of subject

Purkinje image tracker records from 11 subjects with ages varying from 20 to 50 yr showed that backshoots were present in the younger subjects, but consistently absent in the older ones. In addition, overshoots were smaller in the older subjects (Fig. 7). This difference is probably due to the increased mechanical stiffness of the tissues of older eyes. It cannot be explained by mechanical or optical properties of the eye tracker. Overshoots were significantly larger for rightward (abducting) saccades than for leftward saccades [$t(10) = 3.70$, $P = 0.0041$].

DISCUSSION

Our findings support the idea that differences between scleral search coil records and Purkinje image tracker records reflect movements of the lens relative to the rest of the eye during saccades. As hypothesized in the Introduction, there is both a lag of the lens at the start of a saccade (corresponding to our measured backshoots), and an overshoot at the end (corresponding to our measured overshoots). In between these two events, the lens moves faster than the eye.

Several properties of the backshoots and overshoots deserve comment. First, both types of movements have longer durations with larger magnitudes, suggesting that a viscous load is affecting lens movement as well as an elastic load from the stretching of the zonular fibres (for purely elastic loads durations would have a pendulum-like independence of amplitude). Second, the regression lines for the size vs saccade magnitude functions, for both accommodative states and both

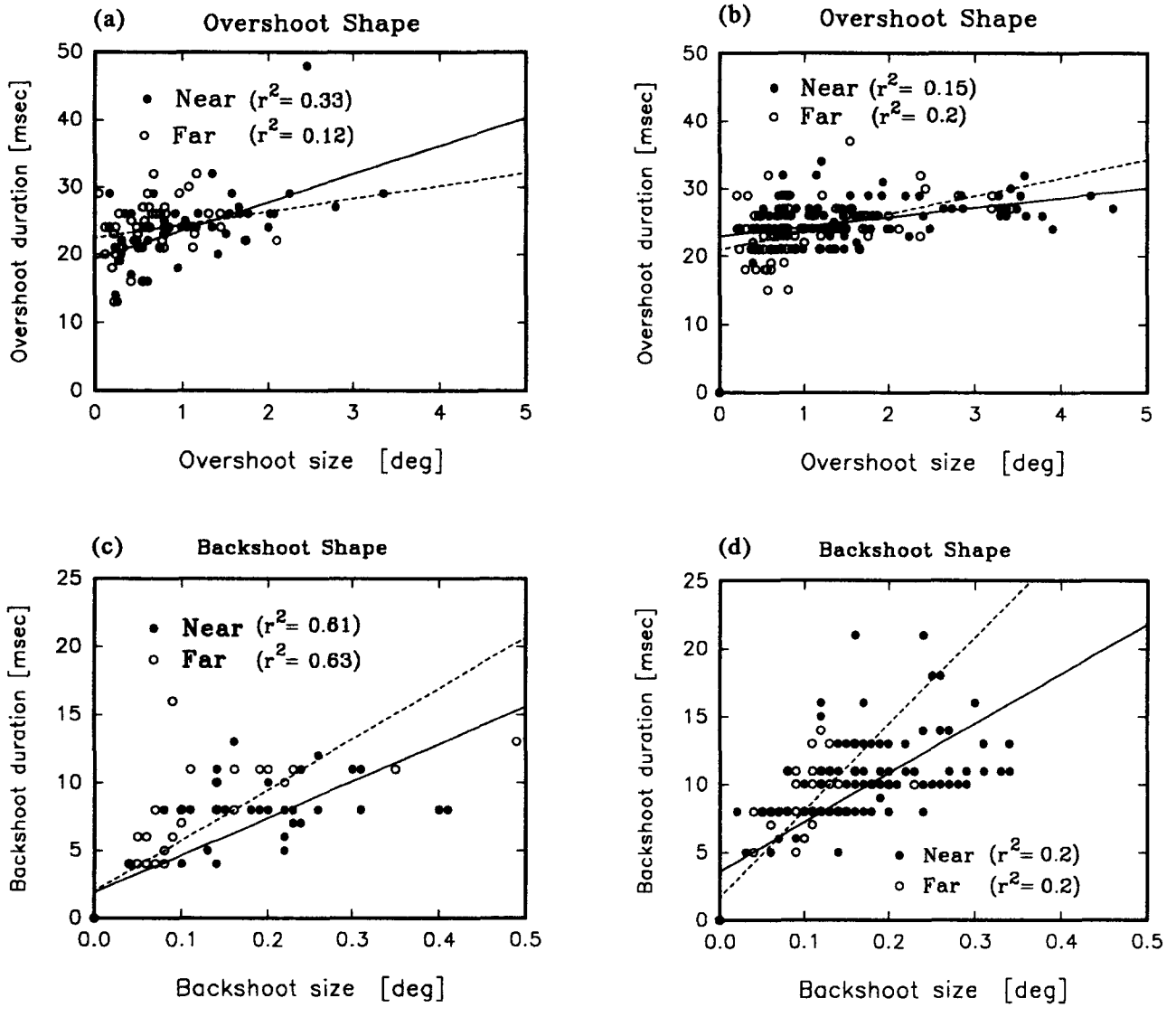

FIGURE 6. Durations of overshoots (a,b) and backshoots (c, d) in subjects IN (a, c) and AM (b, d). Straight lines are linear regressions, performed separately for near (solid lines) and far (dashed lines) accommodations. Positive slopes of the regression lines indicate viscous loads affecting lens movement relative to the eye.

types of movement, have y-intercepts that are greater than zero. This implies that there is some slack in the zonule fibre capsule, allowing the capsule to move slightly before the lens begins to be moved significantly. The "dead zone" can be estimated by summing the y-intercepts of the backshoot and overshoot for each accommodative state. The dead zone for near accommodation is 0.49 deg, and for far is 0.60 deg, suggesting that the flatter lens at far can slip further before meeting noticeable resistance from the zonule. Beyond this zone, however, the flatter lens at distance shows tighter coupling to the eye, as shown in smaller backshoots and overshoots for all sizes of saccade.

Our quantitative measurements of overshoot and backshoot allow us to estimate the actual movement of the retinal image during a saccade, as distinct from the movement of the limbus or of the lens (see Appendix). Using mean values for the overshoot and backshoot for an intermediate accommodative state of 1.25 D provides a picture of the deviations of the image position from the limbus rotational position for a typical saccade (Fig. 8). The initial deviation is nearly as large as the final one, though the rapid initial acceleration of the eye obscures the deviation as reflected in our measured backshoots. At the end of a saccade, a slower approach of the eye to its final position (post-saccadic drift) may partially compensate for the overshoot of the lens within the eye.

Another consequence of lens changes during accommodation is that the back surface of the eye changes its shape. This will change the gain of the fourth Purkinje image's location as a function of rotatory eye position; the function will be steeper at near accommodation than at far, because at near the rear lens surface is more strongly curved. Thus calibrations of the Purkinje image tracker are valid for only one accommodative state.

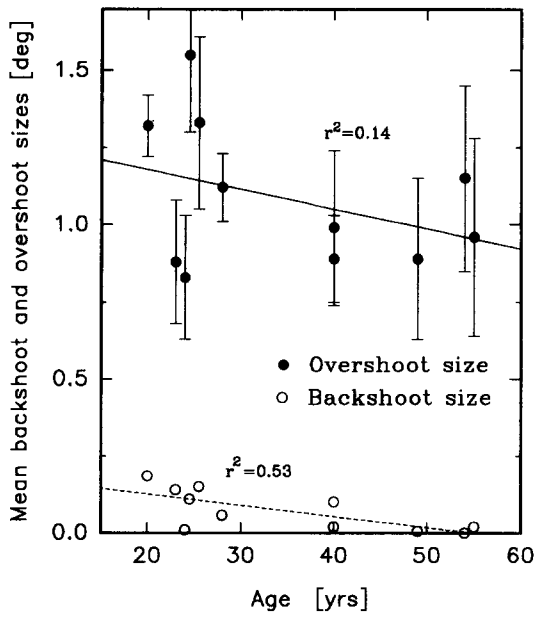

FIGURE 7. Mean overshoot and backshoot sizes vs age of subject. Each subject contributes two points, one for overshoots and one for backshoots. Backshoots are seldom seen in older subjects. Their variability can not be reported accurately because of rounding effects in collecting the data. Error bars for overshoots are ±SD, 20 observations per subject. Viewing distance was 80 cm.

Finally, the observation that overshoots and backshoots decrease in magnitude with age indicates that the reduced flexibility of the lens with age (and possibly the reduced elasticity of other ocular components as well) results in less movement of the lens relative to the eye during saccades. The whole structure becomes more stable. We come to the reassuring conclusion that at least something improves with age.

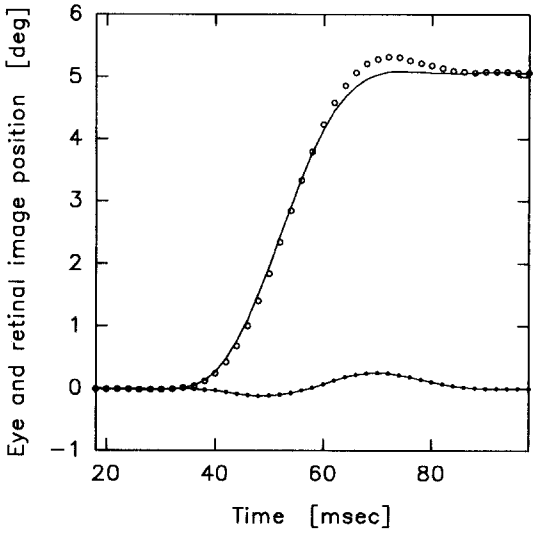

FIGURE 8. Retinal image position (open circles) as a function of time during a saccade (solid line), taking into account the deviation in image position due to movement of the lens off the optical centreline of the eye during saccadic accelerations. The solid dots represent the difference between eyeball and retinal image rotation. The retinal image position is estimated by assuming that each degree of deviation of the eyetracker record from the eyeball rotation signals a displacement of the retinal image of 0.1 deg (see Appendix). Lens deviation has the result of delaying the displacement of the retinal image for a few msec after the limbus begins to move, and of making the retinal image overshoot the target briefly at the end of the saccade.

The dual-Purkinje image eyetracker provides a non-invasive method for determining static eye position during fixation or pursuit with high accuracy and low noise. However, our study demonstrates that, due to the biological properties of the eye, the system is not suitable for the analysis of saccade dynamics (main sequence) and of post-saccadic events such as saccadic dynamic overshoots and post-saccadic drift. Since the effects demonstrated are close to the behaviour of an overdamped mass-spring system, it is likely that most of the eye movement signal can be restored by adaptive inverse filtering (Deubel, in preparation).

Our findings hint at potential problems in the context of certain experimental paradigms. For example, the Purkinje tracker has been frequently used for investigating perceptual processes with stabilized images (e.g. Kelly, 1979). Our data demonstrate that even for small saccades the difference between eye rotation and tracker signal is considerable; this may explain the occasional reappearance of the faded images after small saccades reported in the literature (e.g. Arend & Timberlake, 1986). Since the end of the saccade is veiled by the lens overshoot, experiments with stimulus-contingent displays, especially those that include the manipulation of the stimulus after the saccade, require due care.

Our analysis indicates that during a saccade, movements of the eyeball and of the retinal image may dissociate by up to 0.4 deg for 12 deg saccades, and probably more for larger saccades (Fig. 8). This has to be considered in the interpretation of experiments that analyse the localization of flashed stimuli presented during or shortly after saccades. Finally, the question arises whether the retinal image movement induced by the lens motion at the end of the saccade may affect perceptual or motor processing. There is indeed ample evidence that information intake immediately after the saccade is of considerable importance for processes such as the programming of correction saccades (Deubel, Wolf & Hauske, 1982) or reading (Rayner & Pollatsek, 1987). From our data we estimate the maximum velocity of retinal slip to be up to 15–20 deg/sec for a 12 deg saccade. Average slip amplitude should be < 0.2 deg and last shorter than 30 msec after the end of the saccade. Therefore, interference such as saccadic suppression seems quite unlikely, and is probably limited to very high spatial frequency information in the display.

REFERENCES

Arend, L. E. & Timberlake, G. T. (1986). What is psychophysically perfect image stabilization? Do perfectly stabilized images always disappear? *Journal of the Optical Society of America A, 3*, 235–241.

Bahill, A. T., Brockenbrough, A. & Troost, B. T. (1981). Variability and development of a normative data base for saccadic eye movements. *Investigative Ophthalmology and Visual Science, 21*, 116–125.

Coccius, A. (1888). *Bericht der Internationales Ophthalmologie Kong, Heidelberg, 197*, 199.

Cornsweet, T. N. & Crane, H. D. (1973). Accurate two-dimensional eye tracker using first and fourth Purkinje images. *Journal of the Optical Society of America, 63*, 921–928.

Crane, J. D. & Steele, C. M. (1978). Accurate three-dimensional eyetracker. *Applied Optics, 17*, 691–705.

Crane, H. D. & Steele, C. M. (1985). Generation-V dual-Purkinje-Image eyetracker. *Applied Optics, 24*, 527–537.

Deubel, H., Wolf, W. & Hauske, G. (1982). Corrective saccades: Effect of shifting the saccade goal. *Vision Research, 22*, 353–364.

von Hess, C. (1896). *Greafe's Archiv, 42.*

Kelly, D. H. (1979). Motion and vision. I. Stabilized images of stationary gratings. *Journal of the Optical Society of America, 69*, 1266–1274.

Le Grand, Y. & El Hage, S. G. (1980). *Physiological optics*. Berlin: Springer.

Rayner, K. & Pollatsek, A. (1987). Eye movements in reading: A tutorial review. In Coltheart, M. (Ed.), *Attention and performance XII: The psychology of reading* (pp. 327–362). London: Erlbaum.

van Rensbergen, J., De Troy, A., Cavegn, D., De Graf, P., van Diepen, P. & Fias, W. (1993). The consequences of eye-lens movement during saccades for a stable retinal image. Poster presented at the *Seventh European Conference on Eye Movements*, Durham, 31 August–3 September 1993.

Robinson, D. A. (1963). A method for measuring eye movements using a scleral search coil in a magnetic field. *IEEE Transactions Biomedical Engineering, 26*, 37–145.

Acknowledgements—We thank Johan van Rensbergen and Daniel Cavegn for illuminating discussions, and Ingo Paprotta for serving as a subject and for his valuable aid in the analysis of the data.

APPENDIX

The formation of the four Purkinje images is described in detail by Cornsweet and Crane (1973). The first Purkinje image is formed by light reflected from the front of the cornea (Fig. A1). The cornea has a radius of curvature of about 7.8 mm, with the centre C_1 located about 6 mm from the centre of eye rotation C_r. The fourth Purkinje image is formed by light reflected from the rear surface of the eye lens, and is located in almost exactly the same plane as the first Purkinje image. A single mirror forming the same real image would have a radius of 5.8 mm with a centre C_4 close to the surface of the cornea, and at a distance of about 13 mm from C_r.

With these approximations, the effect of relative lens displacements on locations of the images formed can be estimated. When the eyeball starts to rotate at the beginning of a saccade, the lens would tend to stay in place due to its inertia, leading to an angular lagging of the axis through the centre of rotation and the lens with respect to the optical axis of the eye. When the eye rotation stops at the end of the saccade, relative lens movement may be a combination of angular axis displacement and a pure lateral shift of the lens.

Figure A1 shows the effects of a relative lens axis rotation by the angle ϕ_L; the optical axis of the eye rotates by ϕ_1. The displacements of the first and fourth Purkinje image then are $S_1 = 6 \sin \phi_1$ and $S_4 = 13 \sin(\phi_1 + \phi_L)$, respectively. The eyetracker records the difference $S_4 - S_1$, which for small angles of rotations is (in mm):

$$S_4 - S_1 \approx 7 \sin \phi_1 + 13 \sin \phi_L.$$

From this it can be easily calculated that a recording artifact of 1 deg (which implies a lateral relative displacement of the fourth Purkinje image of 0.122 mm) would indicate an *angular displacement* of the lens axis by 0.538 deg. Moreover, backshoots would occur when ϕ_L lags behind the eye by more than $0.54 \times \phi_1$.

Pure *lateral* displacements of the eye lens are transformed completely into according shifts of the fourth Purkinje image. The experimental

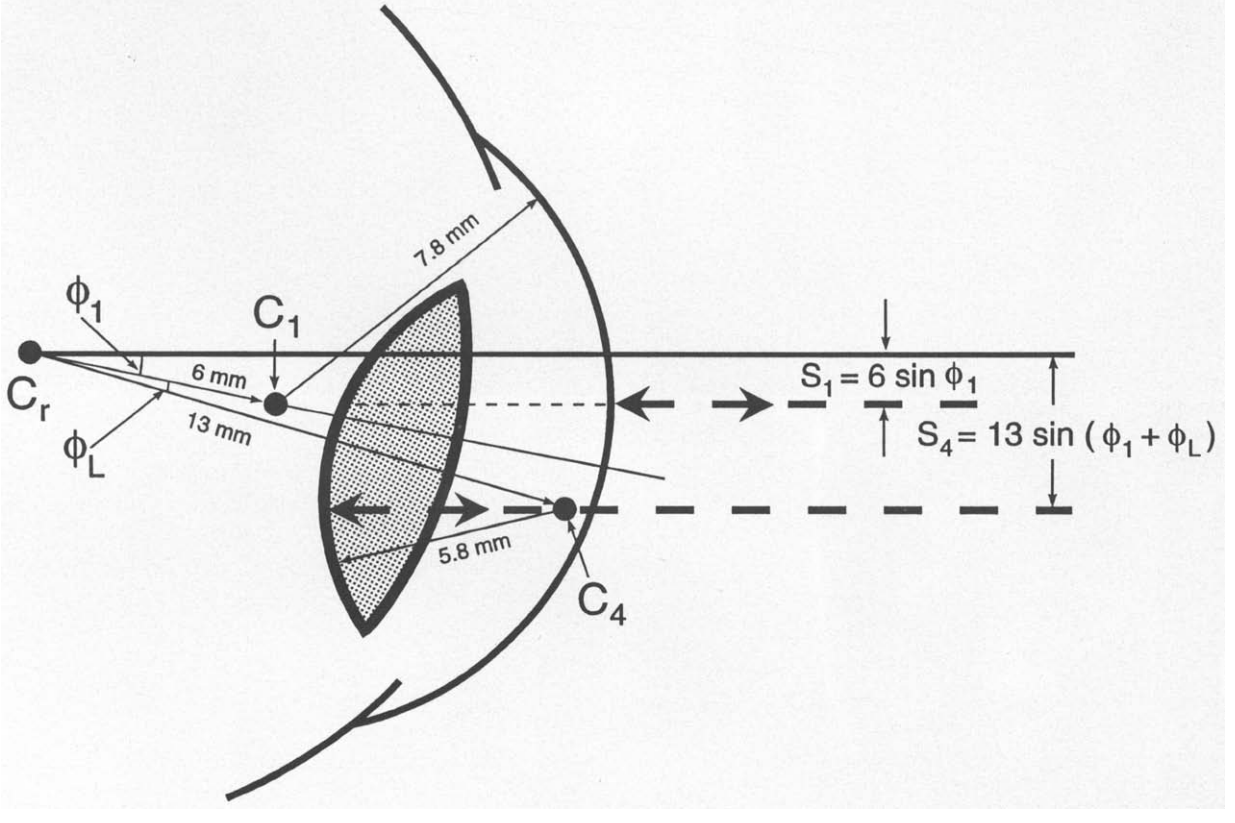

FIGURE A1. Schematic diagram of the eye with cornea and lens. The eyeball is rotated by the angle ϕ_1; the lens overshoots this rotation by the angle ϕ_L. C_r, centre of rotation of the eyeball; C_1, centre of curvature for the cornea; C_4, centre of curvature for the rear surface of the lens; S_1, lateral displacement of the first Purkinje image; S_4, lateral displacement of the fourth Purkinje image.

data in Fig. 5 shows that the sizes of overshoots measured with the eyetracker can reach 4 deg with a 12 deg saccade. According to the calculations presented above this artifact can be due to a lateral lens displacement of 0.488 mm, or to an angular displacement of the axis of the lens of 2.15 deg, or to a combination of both.

Lateral lens displacements lead to shifts of the retinal image. The effect of a lateral displacement d on the visual angle a under which an object appears can be estimated from the focal length of the lens f_L (in the eyeball) which is about 69 mm for the unaccommodated eye (Le Grand & El Hage, 1980). After a lateral lens displacement d, the ray through the centre of the cornea hits the retina at a location displaced by $e = f_L/f_{eye} \times d$, where f_{eye} is the focal length of the simplified eye. For an object at large distance, this is equivalent to an angular change of the line of sight α for which holds:

$$\sin(\alpha) \approx e/f_{eye} = d/f_L.$$

Small angles of rotation yield, finally:

$$\alpha\,[\text{deg}] \approx 360/(2\pi) \times d/f_L = 0.83 \times d\,[\text{mm}].$$

Consequently, the "worst case" of a lens displacement of 0.488 mm as occurring with 12 deg saccades would lead to a shift of visual angle of 0.4 deg.